Department of AERONAUTICS and ASTRONAUTICS
STANFORD UNIVERSITY

AFOSR-66-1755

CLIVE L. DYM
NICHOLAS J. HOFF

PERTURBATION SOLUTIONS FOR THE BUCKLING PROBLEM OF AXIALLY COMPRESSED THIN CYLINDRICAL SHELLS

JULY
1966

The investigation presented in this report was supported by the Air Force Office of Scientific Research under Contract No. AF49(638)-1276

SUDAAR
NO. 282

Department of Aeronautics and Astronautics
Stanford University
Stanford, California

PERTURBATION SOLUTIONS FOR THE BUCK NG PROBLEM OF AXIALLY COMPRESSED THIN CYLINDR. AL SHELLS

by

Clive L. Dym and Nicholas J. Hoff

SUDAAR No. 282
July 1966

The work here reported was performed at Stanford University and sponsored by the U.S. Air Force Office of Scientific Research under contract No. AF 49(638)1276

SUMMARY

A study is made of the effect of initial deviations on the load carrying capacity of thin circular cylindrical shells under uniform axial compression. A perturbation expansion is used to reduce the non-linear equations of von Kármán-Donnell to an infinite set of linear equations, of which only the first few need be solved to obtain a reasonably accurate solution. The results for both infinite shells and shells of finite length indicate that a small imperfection can sharply reduce the maximum load that a thin-walled cylinder will sustain. In addition, for a particular set of boundary conditions, it is shown that the effect of the length, for a finite shell, is small.

THEORY

Governing Equations

The problem under consideration is to determine the effect of initial imperfections on the buckling of a thin circular cylindrical shell under uniform axial compression. Initially the infinite shell will be treated, for which the effects of boundary conditions can be disregarded. Then the discussion will be broadened to include the solution to a shell of finite length with classical simple supports.

The behavior of such a shell, when the deformations are such that non-linear effects are important, is governed by the well-known von Kármán-Donnell Equations. These are two fourth-order, non-linear, coupled, partial differential equations. The first of the equations enforces equilibrium in the radial direction:

$$(D/t)\,\nabla^4(w^* - w_0^*) + \sigma\frac{\partial^2 w^*}{\partial x^{*2}} - \frac{1}{R}\frac{\partial^2 F^*}{\partial x^{*2}} =$$

$$\frac{\partial^2 F^*}{\partial x^{*2}}\frac{\partial^2 w^*}{\partial y^{*2}} - 2\frac{\partial^2 F^*}{\partial x^*\partial y^*}\frac{\partial^2 w^*}{\partial x^*\partial y^*} + \frac{\partial^2 F^*}{\partial y^{*2}}\frac{\partial^2 w^*}{\partial x^{*2}}\ , \qquad (1)$$

where w_0^* is the initial deviation from the perfect cylindrical form, w^* the total radial displacement, σ is the uniform compressive stress applied in the axial direction and positive in compression, F^* is the stress function that assures in-plane equilibrium, and x^* and y^* are, respectively, the axial and circumferential coordinates. The shell wall thickness is denoted by t, the radius by R, Young's modulus is E, Poisson's ratio is ν, and D is the bending rigidity

LIST OF TABLES

Table		Page
1	Variation of Maximum Load Ratio ρ_{max} with the Number of Terms in the Load-Shortening Relationship; Infinite Shell; $\alpha_{20}^{0} = 0.25$	41
2	Comparison of Maximum Load Ratio ρ_{max} and End-Shortening Parameter X for Different Approximations to Load-Shortening Relation	42
3	Comparison of Displacements at Maximum Load	43
4	Comparison of Potential Energy of Various Approximations Up to Maximum Loads	44
5	Variation of Maximum Load Ratio ρ_{max} with the Number of Terms in the Load-Shortening Relationship; Infinite Shell; $\alpha_{20}^{0} = 0.00$	45
6	Influence of Imperfection Size on Maximum Load Ratio of Finite Length Shell	46
7	Variation of Maximum Load Ratio ρ_{max} with Number of Buckles; $L/R = 0.50$	47
8	Variation of Maximum Load Ratio ρ_{max} with Number of Buckles; $L/R = 1.00$	48
9	Variation of Maximum Load Ratio ρ_{max} with Number of Buckles; $L/R = 2.00$	49

LIST OF ILLUSTRATIONS

Figure		Page
1	Generalized Load vs End Shortening	50
2	Typical Load-Shortening Curves	51
3	Maximum Load Ratio ρ_{max} vs Imperfection Amplitude; Non-Symmetric Buckling	52
4	Maximum Load Ratio ρ_{max} vs Imperfection Amplitude; Axisymmetric Buckling	53
5	Maximum Load Ratio ρ_{max} vs Imperfection Amplitude; Comparison with the Results of Koiter and Almroth	54
6	Maximum Load Ratio ρ_{max} vs Half-Length λ	55
7	Maximum Load Ratio ρ_{max} vs Half-Length λ	56

NOTATIONS

A,B,C,D	constants defined in equations (37)
C_{ij}	displacement coefficients defined in equations (21)
D_{ij}	stress function coefficients defined in equations (22)
D	bending rigidity
E	Young's modulus
F^*	stress function (physical)
F	dimensionless stress function
F_i	approximations of i-th order to stress function
G_{ij}	displacement coefficients defined by equations (24)
$G_n(x,y), H_n(x,y)$	functions defined in equations (9) and (8)
I_i	definite integrals in load-shortening relation
L	shell half-length (physical)
$K_1, K_2, \bar{K}_1, \bar{K}_2, J_1, J_2$	constants defined in equations (43)
R	radius of the shell
R_{ij}, P_{ij}	coefficients defined in equations (36)
U	potential energy
U_i	terms in series expansion of U
a	$\frac{1}{\sqrt{2}}(1 - X)^{1/2}$
b	$\frac{1}{\sqrt{2}}(1 + X)^{1/2}$
e	initial displacement amplitude
f	initial displacement form functions

m^*	number of axial half-wave lengths
n^*	number of circumferential buckles
m,n	reduced wave numbers in the axial and circumferential directions, defined in equations (32)
p_i, q_i	roots to Donnell equations, defined in equations (39)
t	shell wall thickness
u^*, v^*	axial and circumferential displacements (physical)
w^*	radial displacement (physical)
w_0^*	initial radial displacement (physical)
w	dimensionless radial displacement
w_0	dimensionless initial displacement
w_i	approximations of i-th order to displacement
x^*, y^*	axial and circumferential physical coordinates
x,y	axial and circumferential dimensionless coordinates
Ω_{ij}	constants defined in equation (241)
$\alpha_{11}^0, \alpha_{20}^0$	initial displacement coefficients
α_{11}, α_{20}	displacement coefficients
α_i, β_i	constants in roots to Donnell equations, equations (39)
β_{11}	stress function coefficient
ϵ	average unit end-shortening
$\epsilon_{x_o}, \epsilon_{y_o}$	axial and circumferential midsurface strains
λ_x	dimensionless shell length; for the infinite shell, it is taken as the axial wave length
λ_y	dimensionless shell circumference; for the infinite shell, it is taken as the circumferential wave length

λ	dimensionless shell half-length
ν	Poisson's ratio
ξ	$(1-\chi)^{-1}$
ρ	stress ratio
σ	uniformly applied compressive stress
φ	$(12(1-\nu^2))^{1/2}$
χ	dimensionless end-shortening parameter
χ_{11}, χ_{20}	constants defined in equations (13)

INTRODUCTION

The determination of the buckling and postbuckling behavior of a thin circular cylindrical shell under uniform axial compression is one of the most challenging problems of the theory of elasticity. The earliest work, that of Lorenz [1], Timoshenko [2], Southwell [3], and Flügge [4] had been concerned with the generation of stability limits. The lack of agreement between these results and experiments conducted during the 1930's led Donnell [5] and von Karman and Tsien [6] to investigate non-linear postbuckling equilibrium. They demonstrated the existence of equilibrium positions at stresses well below the classical value of the buckling stress, and thus were able to offer a partial explanation of the low loads obtained in the laboratory. Since that time many investigators have contributed to the theory; a summary of these efforts has been given in a recent survey paper by Hoff [7]. It is of interest for the present study to take special note of two aspects of the previous work.

The importance of initial inaccuracies in the shape of the cylindrical shell has been recognized for a long time. It had already been studied by Flügge in 1932 and Donnell in 1934. Then in 1950 Donnell and Wan [8] made an extensive investigation of the effects of imperfections. Unfortunately, however, their results may be viewed with some suspicion for in using a minimization principle, they minimized with respect to the displacement coefficients defining the initial shape as well as the total deflection. Thus the system whose total potential was minimized changed its initial configuration during the minimization. The same error is found in articles of Loo [9], Lee [10], and Sobey [11].

This error was avoided in an investigation by Madsen and Hoff [12]. They clearly showed that small imperfections can have a significant effect on the maximum load that the shell can carry. This maximum load, incidentally, is the only quantity that can be observed directly in a test in the laboratory. Further calculations by Almroth [13] and Koiter [14], for axisymmetric imperfections, show similar features. Koiter's paper is a continuation of an ingenious thesis [15] printed in 1945 in which the principal features of postbuckling behavior were derived from the properties of the state of the shell at the critical point of the small-displacement theory. This long-ignored work, in which the significance of the initial deviations was fully demonstrated for the first time, became better known only after a summary of it was published in English [16] in 1963.

It is also interesting to discuss the methods employed by previous investigators to obtain their solutions. With only a few exceptions, beginning with the early investigations of Donnell and von Kármán and Tsien, one of the variational principles of mechanics has been used, generally that of the Minimum of the Total Potential. The most notable of the exceptions is Koiter's analysis of 1945 [15]. More recently, Mayers and Rehfield [17] used the Reissner variational principle, while Almroth [13] linearized the von Kármán-Donnell equations and reduced them to ordinary differential equations before integrating the final equations numerically on a high speed computer. Koiter [14] used a Galerkin procedure on the equation of equilibrium after satisfying the compatibility condition. This is similar to a Rayleigh-Ritz procedure. However, only one term of the displacement series was obtained. It is

worthwhile to note that even when a technique as powerful as the Minimum of the Total Potential Energy is used, a great deal of numerical work on a high speed digital computer is generally required to obtain numerical results.

In this paper the effect of imperfections on the buckling load of a shell will be studied with the aid of a perturbation technique. An approach of this type has enjoyed great prominence in other areas of mathematical physics, especially in fluid mechanics [18]. Few attempts have been made to use this technique in stability problems. Stein [19] has investigated the postbuckling behavior of simply-supported elastic plates, and Kaplan and Fung [20] have analysed the buckling of shallow spherical caps, using perturbation techniques. In both cases non-linear systems of equations were reduced to a tractable form so that results could be obtained in a simpler fashion than previously. In addition, good agreement has been reached with only one or two terms of the expansion.

In the present problem a perturbation expansion, using as the perturbation parameter a characteristic amplitude of the initial deflection, has been used to reduce the nonlinear von Kármán-Donnell equations to an infinite set of linear partial differential equations. Only the first few of these need to be solved in order to obtain a reasonably accurate solution. Investigations are made for the infinite shell and for a shell of finite length with classical simple supports.

For the infinite shell, closed form solutions are given for the deflection function up to the third order of approximation. For the finite shell the satisfaction of the boundary conditions complicates the

problem somewhat, and after two approximations it becomes necessary to resort to a computer to obtain terms of a higher order.

It is shown that the effect of imperfections is significant, and goes a long way towards explaining the lower buckling loads obtained by many experimentalists. Indications are also presented of the catastrophic failure of relatively well made shells which may buckle at high loads.

THEORY

Governing Equations

The problem under consideration is to determine the effect of initial imperfections on the buckling of a thin circular cylindrical shell under uniform axial compression. Initially the infinite shell will be treated, for which the effects of boundary conditions can be disregarded. Then the discussion will be broadened to include the solution to a shell of finite length with classical simple supports.

The behavior of such a shell, when the deformations are such that non-linear effects are important, is governed by the well-known von Kármán-Donnell Equations. These are two fourth-order, non-linear, coupled, partial differential equations. The first of the equations enforces equilibrium in the radial direction:

$$(D/t)\,\nabla^4(w^* - w_0^*) + \sigma \frac{\partial^2 w^*}{\partial x^{*2}} - \frac{1}{R}\frac{\partial^2 F^*}{\partial x^{*2}} =$$

$$\frac{\partial^2 F^*}{\partial x^{*2}}\frac{\partial^2 w^*}{\partial y^{*2}} - 2\frac{\partial^2 F^*}{\partial x^* \partial y^*}\frac{\partial^2 w^*}{\partial x^* \partial y^*} + \frac{\partial^2 F^*}{\partial y^{*2}}\frac{\partial^2 w^*}{\partial x^{*2}}\,, \qquad (1)$$

where w_0^* is the initial deviation from the perfect cylindrical form, w^* the total radial displacement, σ is the uniform compressive stress applied in the axial direction and positive in compression, F^* is the stress function that assures in-plane equilibrium, and x^* and y^* are, respectively, the axial and circumferential coordinates. The shell wall thickness is denoted by t, the radius by R, Young's modulus is E, Poisson's ratio is ν, and D is the bending rigidity

$$D = \frac{Et^3}{12(1-\nu^2)} \quad .$$

The second equation is a compatibility relationship that ensures the continuity of the shell displacements:

$$\nabla^4 F^* + (E/R)\frac{\partial^2 w^*}{\partial x^{*2}} - (E/R)\frac{\partial^2 w_0^*}{\partial x^{*2}} = E\left[\left(\frac{\partial^2 w^*}{\partial x^* \partial y^*}\right)^2 - \frac{\partial^2 w^*}{\partial x^{*2}}\frac{\partial^2 w^*}{\partial y^{*2}} - \left(\frac{\partial^2 w_0^*}{\partial x^* \partial y^*}\right)^2 + \frac{\partial^2 w_0^*}{\partial x^{*2}}\frac{\partial^2 w_0^*}{\partial y^{*2}}\right] \quad . \tag{2}$$

Through the introduction of suitable dimensionless quantities, these two equations can be recast in the following form:

$$\nabla^4 w + 2\rho\, w_{,xx} - F_{,xx} = \nabla^4 w_0 + \varphi[F_{,xx}w_{,yy} - 2F_{,xy}w_{,xy} + F_{,yy}w_{,xx}] \tag{3a}$$

and

$$\nabla^4 F + w_{,xx} = w_{0,xx} + \varphi[w_{,xy}^2 - w_{,xx}w_{,yy} - w_{0,xy}^2 + w_{0,xx}w_{0,yy}] \, , \tag{3b}$$

where

$$x = \frac{x^*}{R}\sqrt{\frac{2E}{\sigma_{cl}}} \, , \quad y = \frac{y^*}{R}\sqrt{\frac{2E}{\sigma_{cl}}} \, , \quad w = \frac{w^*}{t} \, ,$$

$$F = \frac{2}{Rt\sigma_{cl}} F^* \, , \quad \rho = \sigma/\sigma_{cl} \, , \quad \varphi = \sqrt{12(1-\nu^2)} \, ,$$

and

$$\sigma_{cl} = \frac{Et}{\sqrt{3(1-\nu^2)}\, R} \, ,$$

and subscripts after a comma denote differentiation. It is easily seen that the only free parameter remaining in the equations is ρ, the ratio of the buckling stress to the classical critical stress.

The relationship between the applied stress and the average shortening of the shell in the axial direction will next be given. If an average unit end-shortening ϵ is defined by

$$\epsilon = -\frac{1}{4\pi RL}\int_0^{2\pi R}\int_{-L}^{L}\frac{\partial u^*}{\partial x^*}\,dx^*dy^* \quad ,$$

then by means of the midsurface strain-displacement relationship in the x^* direction

$$\epsilon_{x_0} = \frac{\partial u^*}{\partial x^*} + \frac{1}{2}\left(\frac{\partial w^*}{\partial x^*}\right)^2$$

and the stress-strain law

$$\epsilon_{x_0} = -\frac{\sigma}{E} + \frac{1}{E}\left(\frac{\partial^2 F^*}{\partial y^{*2}} - \nu\frac{\partial^2 F^*}{\partial x^{*2}}\right)$$

the load-shortening relationship can be written, with the introduction of the dimensionless quantities defined earlier, as

$$\frac{\sigma R}{Et} = \frac{\epsilon R}{t} + \frac{1}{\lambda_x\lambda_y}\int_0^{\lambda_y}\int_{-\frac{\lambda_x}{2}}^{\frac{\lambda_x}{2}}\left[F_{,yy} - \nu F_{,xx} - \frac{\varphi}{2}w_{,x}^2 + \frac{\varphi}{2}w_{0,x}^2\right]dxdy \quad , \quad (4)$$

where

$$\lambda_x = \frac{2L}{R}\sqrt{\frac{2E}{\sigma_{cl}}} \quad , \quad \lambda_y = 2\pi\sqrt{\frac{2E}{\sigma_{cl}}} \quad .$$

This is recast once more into a slightly more convenient form:

$$\rho = \chi + \frac{\sqrt{3(1-\nu^2)}}{\lambda_x \lambda_y} \int_0^{\lambda_y} \int_{-\frac{\lambda_x}{2}}^{\frac{\lambda_x}{2}} [F_{,yy} - \nu F_{,xx} - \frac{\varphi}{2} w_{,x}^2 + \frac{\varphi}{2} w_{0,x}^2] dx dy, \quad (4a)$$

where

$$\rho = \sqrt{3(1-\nu^2)}\ \frac{\sigma R}{Et} = \sigma/\sigma_{cl}$$

$$\chi = \sqrt{3(1-\nu^2)}\ \frac{\epsilon R}{t} = \epsilon/(\sigma_{cl}/E) = \epsilon/\epsilon_{cl} \ . \quad (4b)$$

Method of Solution

A perturbation expansion will be used to reduce the nonlinear equations given above to an infinite system of linear equations, only the first few of which need to be solved to obtain a reasonably accurate solution. Since the primary interest is in determining the effect of imperfections on the load-carrying capacity of a shell, it seems natural to choose as a perturbation parameter some quantity which would be indicative of the degree to which the shell's form deviates from the perfect circular cylinder. With this in mind, the initial deviation was taken as

$$w_0 = e\ f(x,y) \ ,$$

where $f(x,y)$ represents the shape of the initial deformation, and e is a characteristic amplitude. As the displacements have been nondimensionalized with respect to the shell thickness, the number e actually represents the deviation amplitude as a fraction (or multiple) of the

thickness. There is one restriction placed on the form function, $f(x,y)$, i.e., it must satisfy appropriate boundary conditions in those investigations where shells of finite length are examined.

Then the characteristic amplitude $\underline{e}$ is taken as the perturbation parameter and it is assumed that the radial displacement w and the stress function F can be represented by the following power series in $\underline{e}$:

$$w = \sum_{n=1} w_n(x,y)e^n \tag{6a}$$

$$F = \sum_{n=1} F_n(x,y)e^n \quad . \tag{6b}$$

It would seem then that all that would be needed to effect the desired solution would be to substitute the expansions (6) into the differential equations (3) and carry forward the linearization procedure. Then the first few terms of the expansions can be obtained and used with equation (4) or (4a) to generate the desired relation between the load and the end-shortening. Unfortunately, the results obtained thusly would be spurious.

The curve generated in this fashion would have no true maximum (curve S, Figure 1); rather it would approach the line $\rho = 1$ asymptotically as the shortening parameter X approaches infinity. This does not at all resemble the type of behavior expected for a circular cylindrical shell, with imperfections, under axial compression.

Fortunately this unexpected result can be both explained and remedied. What the expansion has accomplished in the above approach has been the movement of the singular point of the load-shortening curve

from the region around $\rho = \chi = 1$ in such a way that now χ becomes infinite as ρ approaches unity. The singular nature of the load-shortening at $\rho = \chi = 1$ is evident from the cusp in the curve (for the perfect shell) at that point (Figure 1). The correction of the above fallacious results would seem to lie, then, in expanding the load parameter ρ about the shortening parameter χ, and indeed, a natural form of this expansion is available from the load shortening relationship (4a).

If the expansions (6) for the displacement w and the stress function F are substituted into the functional on the right-hand side of (4a), the load-shortening relation can be written in the following way:

$$\rho = \chi + eI_1 + e^2 I_2 + \ldots + e^n I_n \tag{7}$$

where

$$I_1 = \frac{\sqrt{3(1-\nu^2)}}{\lambda_x \lambda_y} \int_0^{\lambda_y} \int_{-\lambda}^{+\lambda} (F_{1,yy} - \nu F_{1,xx}) dxdy \tag{7a}$$

$$I_2 = \frac{\sqrt{3(1-\nu^2)}}{\lambda_x \lambda_y} \int_0^{\lambda_y} \int_{-\lambda}^{+\lambda} (F_{2,yy} - \nu F_{2,xx} - \frac{\varphi}{2} w_{1,x}^2 + \frac{\varphi}{2} f_{,x}^2) dxdy \tag{7b}$$

$$I_3 = \frac{\sqrt{3(1-\nu^2)}}{\lambda_x \lambda_y} \int_0^{\lambda_y} \int_{-\lambda}^{+\lambda} (F_{3,yy} - \nu F_{3,xx} - \varphi w_{1,x} w_{2,x}) dxdy \tag{7c}$$

$$I_4 = \frac{\sqrt{3(1-\nu^2)}}{\lambda_x \lambda_y} \int_0^{\lambda_y} \int_{-\lambda}^{+\lambda} (F_{4,yy} - \nu F_{4,xx} - \frac{\varphi}{2} w_{2,x}^2 - \varphi w_{1,x} w_{3,x}) dxdy \tag{7d}$$

and so on, where $\lambda = \lambda_x/2$.

Then the expansion (7) will be used in conjunction with the expansions (6) to linearize the nonlinear differential equations (3).

It is also possible, and enlightening, to argue the use of the expansion (7) from two other points of view. The final aim of any such analysis of the nonlinear behavior of the circular cylindrical shell under uniform axial compression is usually the determination of the load-shortening relationship for the shell. As can be seen here from equation (7), this relationship displays the load parameter ρ as a power series in the imperfection amplitude $\underline{e}$. Thus it would seem consistent to replace ρ in the differential equation with its corresponding power series, in much the same fashion as was done for the stress function F and the displacement w by their expansions (6).

Further, the behavior expected is illustrated by the dashed lines in Figure 1. It is seen here that the maxima sought are relatively close to the straight line $\rho = \chi$. Thus it would seem only natural when linearizing the governing differential equations to perturb about this line at the same time.

Both of these arguments are helpful for an understanding of the problem and its solution; it should be remembered, however, that the primary purpose of the expansion for ρ is to keep the appropriate mathematical behavior in the region where it belongs.

The expansions given can now be substituted in the differential equations to obtain, as mentioned earlier, the equivalent infinite set of linearized equations. The first few of these are presented here:

$$O(e) \quad \nabla^4 w_1 + 2\chi w_{1,xx} - F_{1,xx} = \nabla^4 f$$

$$\nabla^4 F_1 + w_{1,xx} = f_{,xx} \tag{8a}$$

$$O(e^2) \quad \nabla^4 w_2 + 2\chi w_{2,xx} - F_{2,xx} = -2I_1 w_{1,xx} + \varphi[F_{1,xx} w_{1,yy}$$

$$- 2F_{1,xy} w_{1,xy} + F_{1,yy} w_{1,xx}]$$

$$\nabla^4 F_2 + w_{2,xx} = \varphi[w_{1,xy}^2 - w_{1,xx} w_{1,yy} - w_{0,xy}^2 \tag{8b}$$

$$+ w_{0,xx} w_{0,yy}]$$

$$O(e^3) \quad \nabla^4 w_3 + 2\chi w_{3,xx} - F_{3,xx} = - 2I_1 w_{2,xx} - 2I_2 w_{1,xx}$$

$$+ \varphi[F_{1,xx} w_{2,yy} + F_{2,xx} w_{1,yy} - 2F_{1,xy} w_{2,xy}$$

$$- 2F_{2,xy} w_{1,xy} + F_{1,yy} w_{2,xx} + F_{2,yy} w_{1,xx}] \tag{8c}$$

$$\nabla^4 F_3 + w_{3,xx} = \varphi[2w_{1,xy} w_{2,xy} - w_{1,xx} w_{2,yy} - w_{2,xx} w_{1,yy}].$$

This sequence of equations may be written in the form:

$$O(e^n) \quad \nabla^4 w_n + 2\chi w_{n,xx} - F_{n,xx} = G_n(x,y) \tag{9a}$$

$$\nabla^4 F_n + w_{n,xx} = H_n(x,y) \ , \tag{9b}$$

where $G_n(x,y)$ and $H_n(x,y)$ are made up of products and squares of the preceding (n-1) terms. It is in these expressions that the nonlinearity of the original system is preserved, although as a higher order effect (as it should properly be for this investigation), in a form that is tractable.

The pair of equations (9) can be uncoupled, i.e., the stress function $F_n(x,y)$ can be eliminated between these two equations to yield a single partial differential equation in terms of the radial displacement $w_n(x,y)$:

$$\nabla^8 w_n + 2\chi \nabla^4 w_{n,xx} + w_{n,xxxx} = \nabla^4 G_n + H_{n,xx} \ .$$

This equation is reminiscent of the linearized equation of Donnell (which can be obtained from the nonlinear von Kármán-Donnell equations by omitting the nonlinear terms), but now the load parameter ρ has been replaced with the shortening parameter χ, and the equation is inhomogeneous.

The Question of Covergence

The mathematical foundations of perturbation theory are not yet completely established. There is, at this time, no general technique or theorem to indicate the range of validity of an asymptotic or perturbation expansion. Thus the engineer must, in general, rely on physical evidence, in the form of, say, experimental results, or different analytical approaches, in order to ascertain the validity of his solutions.

In addition, the following three indicators seem to have relevant implications, both from the mathematical and the physical points of view.

The first of these centers about the expansion for the radial displacement w:

$$w = ew_1 + e^2 w_2 + \ldots + e^n w_n \ .$$

In a manner similar to the ratio test used in examining the convergence of power series, one can examine the behavior of the ratio $(e\, w_n/w_{n-1})$ in the neighborhood of the maximum load. The use of this indicator, however, should be tempered by the knowledge that immediately after the maximum has been reached, the shell buckles and the displacements become very large. Thus this indicator is useful in the region just before the maximum load.

The second indicator hinges on the earlier argument that the perturbation takes place around the line $\rho = \chi$ at the same time when the governing equations are linearized. Thus an important examination would be to see whether

$$\rho \cong \chi$$

near the maximum load.

The final test has a more physical appeal as it consists of an examination of the potential energy of the system as given by each additional approximation. For the energy too may be written in the form

$$U = U_0 + eU_1 + \ldots e^n U_n$$

and it is reasonable that if the perturbing effect is truly small, the increase in energy because of it should be correspondingly small.

SOLUTIONS

Infinite Shell

The purpose of this section is to illustrate the procedure, described above, for obtaining the maximum loads of imperfect cylindrical shells. The expression "infinite shell" is used to indicate the fact that no attempt is made to satisfy any boundary conditions, and thus only particular integrals are obtained for the differential equations involved. Since displacements and stresses are represented as trigonometric functions, which automatically satisfy requirements of boundedness at infinity, this is a considerable simplification.

In addition, in order to carry out the integrations indicated in equations (7), the quantities λ_x, λ_y are assumed to represent the axial and circumferential wave lengths of one buckle.

The initial deviation is taken in the form

$$w_0 = e(\alpha_{11}^0 \cos mx \cos ny + \alpha_{20}^0 \cos 2mx) \ , \tag{10}$$

where α_{11}^0, α_{20}^0 are displacement coefficients that may be arbitrarily assigned, and m,n are reduced wave numbers.

The first approximation to the total displacement is obtained as the solution of

$$\nabla^8 w_1 + 2\chi \nabla^4 w_{1,xx} + w_{1,xxxx} = \nabla^8 f + f_{,xxxx} \ . \tag{11}$$

A solution is assumed in the form

$$w_1 = \alpha_{11} \cos mx \cos ny + \alpha_{20} \cos 2mx \ , \tag{12}$$

which leads to

$$\alpha_{11} = \frac{\alpha_{11}^0}{1-X/X_{11}} \quad , \quad \alpha_{20} = \frac{\alpha_{20}^0}{1-X/X_{20}} \, , \tag{13}$$

where

$$X_{11} = \frac{m^4+(m^2+n^2)^4}{2m^2(m^2+n^2)^2} \tag{13a}$$

$$X_{20} = \frac{(2m)^4+(2m)^8}{2(2m)^6} \, . \tag{13b}$$

Buckling is likely to take place under the smallest load if the initial deviation pattern is so selected as to make the two denominators in equations (13) vanish simultaneously, as was shown by Madsen and Hoff [12]. Thus the requirement is

$$X_{11} = X_{20} = 1 \tag{14a}$$

which leads to

$$m = n = 1/2 \, . \tag{14b}$$

Then the initial deviation form is

$$f(x,y) = \alpha_{11}^0 \cos \frac{x}{2} \cos \frac{y}{2} + \alpha_{20}^0 \cos x \tag{15}$$

and the first approximation for the radial displacement is

$$w_1 = \xi(\alpha_{11}^0 \cos \frac{x}{2} \cos \frac{y}{2} + \alpha_{20}^0 \cos x) \, , \tag{16}$$

where

$$\xi = (1-X)^{-1} \, . \tag{16a}$$

The corresponding stress function F_1 is found from

$$\nabla^4 F_1 = - w_{1,xx} + f_{,xx} . \tag{17}$$

After substitution from (15), (16) one finds easily that

$$F_1 = -(1-\xi)f(x,y) . \tag{18}$$

Now it is possible to calculate from equations (7) the first approximation to the load-shortening relation. Equation (18) indicates that F_1 is periodic, and so indeed will be all the succeeding approximations to the stress function. In view of this, the integrals of (7) can be recast as:

$$I_1 = 0 \tag{19a}$$

$$I_2 = - \frac{\varphi\sqrt{3(1-\nu^2)}}{2\lambda_x\lambda_y} \int_0^{\lambda_x}\int_0^{\lambda_y} (w_{1,x}^2 - f_{,x}^2)dxdy \tag{19b}$$

$$I_3 = - \frac{\varphi\sqrt{3(1-\nu^2)}}{\lambda_x\lambda_y} \int_0^{\lambda_x}\int_0^{\lambda_y} (w_{1,x}w_{2,x})\, dxdy \tag{19c}$$

$$I_4 = - \frac{\varphi\sqrt{3(1-\nu^2)}}{2\lambda_x\lambda_y} \int_0^{\lambda_x}\int_0^{\lambda_y} (w_{2,x}^2 + 2w_{1,x}w_{3,x})dxdy . \tag{19d}$$

Then the first approximation to the load-shortening equation is obtained as

$$\frac{\sigma R}{Et} = \frac{\epsilon R}{t} - \frac{\sqrt{3(1-\nu^2)}e^2}{16} \frac{\chi(2-\chi)}{(1-\chi)^2} [(\alpha_{11}^0)^2 + 8(\alpha_{20}^0)^2] . \tag{20}$$

One can proceed in a similar fashion to calculate further approximations. In the present analysis results were obtained up to the third order approximation for the displacement, and the results are given below:

$$w_2 = C_{11} \cos\frac{x}{2} \cos\frac{y}{2} + C_{31} \cos\frac{3x}{2} \cos\frac{y}{2} + C_{20} \cos x + C_{02} \cos y, \quad (21a)$$

where

$$C_{11} = \frac{1}{2}\sqrt{3(1-\nu^2)}\,(\alpha_{11}^0\alpha_{20}^0)(3\xi^3 - 2\xi^2 - \xi) \quad (21b)$$

$$C_{31} = \sqrt{3(1-\nu^2)}\,(\alpha_{11}^0\alpha_{20}^0)\left(\frac{59\xi^3 - 50\xi^2 - 9\xi}{450 + 256\xi}\right) \quad (21c)$$

$$C_{20} = \frac{1}{32}\sqrt{3(1-\nu^2)}\,(\alpha_{11}^0)^2(3\xi^3 - 2\xi^2 - \xi) \quad (21d)$$

$$C_{02} = \frac{1}{8}\sqrt{3(1-\nu^2)}\,(\alpha_{11}^0)^2(\xi^2 - \xi)\,, \quad \text{and} \quad , \quad (21e)$$

$$F_2 = D_{11} \cos\frac{x}{2} \cos\frac{y}{2} + D_{31} \cos\frac{3x}{2} \cos\frac{y}{2} + D_{20} \cos x + D_{02} \cos y, \quad (22a)$$

where

$$D_{11} = C_{11} - \sqrt{3(1-\nu^2)}\,(\alpha_{11}^0\alpha_{20}^0)(\xi^2 - 1) \quad (22b)$$

$$D_{31} = \frac{9}{25} C_{31} - \frac{1}{25}\sqrt{3(1-\nu^2)}\,(\alpha_{11}^0\alpha_{20}^0)(\xi^2 - 1) \quad (22c)$$

$$D_{20} = C_{20} - \frac{1}{16}\sqrt{3(1-\nu^2)}\,(\alpha_{11}^0)^2(\xi^2 - 1) \quad (22d)$$

$$D_{02} = -\frac{1}{16}\sqrt{3(1-\nu^2)}\,(\alpha_{11}^0)^2(\xi^2 - 1)\,. \quad (22e)$$

For the second order approximation in w, the load-shortening relation becomes:

$$\frac{\sigma R}{Et} = \frac{\epsilon R}{t} - \frac{1}{16}\sqrt{3(1-\nu^2)}\left\{e^2\ \frac{\chi(2-\chi)}{(1-\chi)^2}\left[(\alpha_{11}^0)^2 + 8(\alpha_{20}^0)^2\right]\right.$$

$$\left. + 2e^3\ \frac{1}{1-\chi}\left[\alpha_{11}^0\ C_{11} + 8\alpha_{20}^0\ C_{20}\right]\right\}\ . \qquad (23)$$

The third order displacement function has nine harmonics:

$$w_3 = G_{11}\cos\frac{x}{2}\cos\frac{y}{2} + G_{20}\cos x + G_{02}\cos y + G_{22}\cos x\cos y$$

$$+ G_{13}\cos\frac{x}{2}\cos\frac{3y}{2} + G_{31}\cos\frac{3x}{2}\cos\frac{y}{2} + G_{40}\cos 2x +$$

$$+ G_{42}\cos 2x\cos y + G_{51}\cos\frac{5x}{2}\cos\frac{y}{2}\ , \qquad (24a)$$

where

$$G_{11} = I_2\xi^2\alpha_{11}^0 + \frac{1}{2}\sqrt{3(1-\nu^2)}\ \xi[\alpha_{11}^0\ \Omega_{02} + \alpha_{11}^0\ \Omega_{20} + \xi\alpha_{11}^0 C_{02}$$

$$+ \xi\alpha_{11}^0 C_{20} + \alpha_{20}^0\Omega_{31} + \alpha_{20}^0\Omega_{11} + \xi\alpha_{20}^0 C_{31} + \xi\alpha_{20}^0 C_{11}] \qquad (24b)$$

$$G_{20} = I_2\xi^2\alpha_{20}^0 + \frac{1}{16}\sqrt{3(1-\nu^2)}\ \xi[\alpha_{11}^0\Omega_{11} + \alpha_{11}^0\Omega_{31} + \xi\alpha_{11}^0 C_{11}$$

$$+ \xi\alpha_{11}^0 C_{31}] \qquad (24c)$$

$$G_{02} = \frac{1}{8}\sqrt{3(1-\nu^2)}\ \alpha_{11}^0\Omega_{11} \qquad (24d)$$

$$G_{22} = \frac{2\sqrt{3(1-\nu^2)}\,\xi}{(8+9\xi)}\left[\alpha_{11}^0\Omega_{31} + 4\alpha_{20}^0\Omega_{02} + \frac{1}{4}\xi\alpha_{11}^0 C_{31} + \xi\alpha_{20}^0 C_{02}\right] \qquad (24e)$$

$$G_{13} = \frac{\sqrt{3(1-\nu^2)}\,\xi}{(50+576\xi)}\left[25\alpha_{11}^0\Omega_{02} + \xi\alpha_{11}^0 C_{02}\right] \qquad (24f)$$

$$G_{31} = \frac{\sqrt{3(1-\nu^2)}\,\xi}{(450+256\xi)} \left[25\alpha^0_{11}\Omega_{20} + 9\xi\alpha^0_{11}C_{20} + 25\alpha^0_{20}\Omega_{11} + 9\xi\alpha^0_{20}C_{11}\right] \quad (24g)$$

$$G_{40} = \frac{\sqrt{3(1-\nu^2)}\,\xi}{(64+72\xi)} \left[4\alpha^0_{11}\Omega_{31} + \xi\alpha^0_{11}C_{31}\right] \quad (24h)$$

$$G_{42} = \frac{\sqrt{3(1-\nu^2)}\,\xi}{(200+441\xi)} \left[\frac{25}{8}\,\alpha^0_{11}\Omega_{31} + \frac{1}{2}\,\xi\alpha^0_{11}C_{31}\right] \quad (24i)$$

$$G_{51} = \frac{\sqrt{3(1-\nu^2)}\,\xi}{[250(169)+8(1296)\xi]} \left[\frac{169}{2}\,\alpha^0_{20}\Omega_{31} + \frac{25}{2}\,\xi\alpha^0_{20}C_{31}\right] , \quad (24j)$$

where

$$I_2 = -\frac{1}{16}\sqrt{3(1-\nu^2)}\,(\xi^2-1)\left[(\alpha^0_{11})^2 + 8(\alpha^0_{20})^2\right] \quad (24k)$$

and

$$\Omega_{ij} = \xi D_{ij} - (1-\xi)C_{ij} \quad . \quad (24l)$$

The load-shortening relationship corresponding to this order of the displacement is

$$\frac{\sigma R}{Et} = \frac{\epsilon R}{t} - \frac{\sqrt{3(1-\nu^2)}}{16}\left\{e^2\,\frac{X(2-X)}{(1-X)^2}\left[(\alpha^0_{11})^2 + 8(\alpha^0_{20})^2\right]\right.$$

$$+ 2e^3\,\frac{1}{(1-X)}\left[\alpha^0_{11}C_{11} + 8\alpha^0_{20}C_{20}\right] + e^4\left[C^2_{11} + 9C^2_{31} +\right.$$

$$\left.\left. + 8C^2_{20} + 2\,\frac{1}{(1-X)}\,\alpha^0_{11}G_{11} + 16\,\frac{1}{1-X}\,\alpha^0_{20}G_{20}\right]\right\} \quad (25)$$

Thus expressions have been derived for the displacement up to the order of $O(e^3)$, and the load-shortening equation to $O(e^4)$. The results are presented in Figures 2 through 4 and Tables 1 through 5. The calculations were carried out on the Burroughs B-5500 Digital Computer at the

Computation Center of Stanford University. Values of e, α_{11}^0, α_{20}^0 were chosen for use with equations (20), (23) and (25). Then the end-shortening parameter X was stepped from zero to unity in intervals of 0.01, and load-shortening curves (Fig. 2) were thus generated. Maxima were easily obtainable from these plots. The results for axisymmetric buckling were obtained by taking $\alpha_{11}^0 = 0$.

The form of the load-shortening curve is shown in Fig. 2. It should be pointed out that the form shown is not reliable beyond the maximum load, because beyond this point the validity of the expansions becomes doubtful. Indeed, an examination of Table 3 shows that the ratio

$$ew_n/w_{n-1}$$

is always small right up to the vicinity of the maximum, and then becomes equal to or greater than one at the maximum load for the smaller imperfections. This latter occurence is not surprising for it can also be seen from this table that the displacement w increases much more rapidly for the smaller imperfections. This implies the possibility of catastrophic failures, in the laboratory, of even well-made specimens.

Table 1 and Fig. 3 show the variation of the maximum load obtained for a given value of the imperfection parameter e with the number of approximations kept in the load-shortening expression, as well as showing the variation of the maximum load with the imperfection parameter. From the viewpoint of "convergence" considerations, there seems to be very good agreement for small values of e, but less agreement as the imperfection becomes greater than one-tenth of the wall-thickness in amplitude. This conclusion is also implicit in the results given in

Table 2, where it is seen that

$$\rho \cong X$$

for small values of $\underline{e}$; but as the imperfection increases, the maxima seem to occur further away from the straight line which reflects the linear solution. Similar remarks may be made with reference to the values of the potential energies of the various approximations which are given in Table 4. Incidentally, the potential energy was obtained by integration of the area under the load-shortening curve.

Plots of maximum load versus imperfection amplitude are presented in Figures 3, 4, and 5. The first of these is a graphical comparison of the results for approximations of different orders for nonsymmetric buckling. Figure 4 shows only the effect of imperfections for axisymmetric buckling. In the latter case it should be noted that the linearization involved in the perturbation technique is such that axisymmetric initial deviations lead to total deformations that are also axisymmetric.

The last figure (Figure 5) is a graphical comparison of results of Almroth [13] and Koiter [14] with results obtained from the present solution for both axisymmetric and non-axisymmetric buckling deformations. The work of these two investigators involved consideration of general buckling deformations, but axisymmetric initial imperfections. From the results of the present analysis alone (curves C, D), it appears that axisymmetric deviations are the more critical. Further, for small values of the imperfection amplitude $\underline{e}$, Koiter's curve (A) is below the curve for general buckling obtained here. The curve obtained by Almroth, which he suggests as a lower bound even for cylinders with non-axisymmetric

initial deformations, bounds the present general solution from below, up to moderately large values (0.35) of the imperfection parameter $\underline{e}$.

In addition, some of the results obtained by Madsen and Hoff [12] are presented here:

e	ρ Madsen and Hoff	ρ Present Analysis
10^{-2}	0.842	0.894
10^{-1}	0.587	0.610
0.5	no maximum	0.151

For the first two cases the difference is much less than 10%. It might be pointed out that although the initial imperfections are the same in the two cases, the total deflected shapes are different because higher order approximations in the perturbation expansion include considerably more harmonics than used by Madsen and Hoff.

As a further analysis of the effect of axisymmetric imperfections, the coefficient α_{20}^{0} was taken to be zero. The results are shown in Table 5. The term of $O(e^3)$ in the load-shortening expression vanishes in this case so that we have fewer values for comparison. However, for both approximations shown, the buckling loads are greater than or equal to those for which an axisymmetric imperfection mode was present.

Finite Shell: SS3 Boundary Conditions

With the perturbation scheme already established, attention is now turned to shells of finite length. The solutions obtained thus far for shells of finite length are eigenvalue solutions to the linearized Donnell equation (see, for example, Hoff [21] and Hoff and Soong [22]).

From these solutions critical stresses and waveforms, but not actual amplitudes, can be obtained.

The approach taken here differs from the analysis in the previous section in that homogeneous solutions to the differential equations are added to the particular integrals to satisfy the boundary conditions.

The boundary conditions considered are those known as SS3 conditions, or, alternatively, the classical simple supports:

$$w = w_{,xx} = \sigma_x = v = 0 \tag{26a}$$

at

$$x = \pm \lambda \, . \tag{26b}$$

Here σ_x is the axial normal stress and v the reduced circumferential displacement that accompany buckling. The quantity λ denotes the dimensionless shell half-length

$$\lambda = [12(1-\nu^2)]^{1/4} \frac{L}{\sqrt{Rt}} \tag{27}$$

where L is the actual (physical) half-length of the shell.

The second two conditions can be recast in terms of the stress function F. It follows from the definition of the stress function that

$$\sigma_x = 0 \quad \text{implies} \quad F_{,yy} = 0. \tag{28}$$

Moreover, in the strain-displacement relation

$$\epsilon_y = \frac{\partial v^*}{\partial y^*} - \frac{w^*}{R} + \frac{1}{2}\left(\frac{\partial w^*}{\partial y^*}\right)^2 ,$$

one has $w = v = 0$ at $x = \pm \lambda$. Hence

$$\epsilon_{y_0} = 0 .$$

On the other hand, from Hooke's law:

$$\epsilon_{y_0} = \frac{1}{E} (\sigma_y - \nu\sigma_x) .$$

But since it was stipulated that $\sigma_x = 0$, and since $\epsilon_{y_0} = 0$ at the ends of the shell, then

$$\sigma_y = 0$$

which implies

$$F,_{xx} = 0 . \tag{28}$$

Thus the four boundary conditions to be satisfied at each end of the shell can be written as

$$w = w,_{xx} = F,_{yy} = F,_{xx} = 0 . \tag{29}$$

The boundary conditions will be used as given in equation (29) since the pairs of differential equations given for each order will be solved in the coupled form as displayed in equations (8).

The equations for the first approximations to the deflections, w_1, and the stress function, F_1, are:

$$\nabla^4 w_1 + 2\chi w_{1,xx} - F_{1,xx} = \nabla^4 f \tag{30a}$$

$$\nabla^4 F_1 + w_{1,xx} = f,_{xx} . \tag{30b}$$

The initial imperfection form function is taken in the form:

$$f(x,y) = \alpha_{11}^0 \cos mx \cos ny , \tag{31}$$

where α_{11}^{0} is a displacement coefficient that may be arbitrarily assigned, and m,n are reduced wave numbers given by

$$m = \frac{m^*\pi}{2[12(1-\nu^2)]^{1/4}} \frac{\sqrt{Rt}}{L}, \quad n = \frac{n^*}{[12(1-\nu^2)]^{1/4}} \sqrt{\frac{t}{R}}, \tag{32}$$

and m^* is the number of axial half-wave lengths, and n^* the number of circumferential buckles.

If solutions are assumed in the form

$$w_1 = \alpha_{11} \cos mx \cos ny \tag{32a}$$

$$F_1 = \beta_{11} \cos mx \cos ny \tag{32b}$$

they will satisfy the differential equations (30) if

$$\alpha_{11} = \frac{\alpha_{11}^{0}}{1 - 2\chi\left[\frac{(m^2+n^2)^2}{m^2} + \frac{m^2}{(m^2+n^2)^2}\right]^{-1}} \tag{33a}$$

$$\beta_{11} = \frac{2\chi\alpha_{11}^{0}}{\frac{(m^2+n^2)^4}{m^4} + 1 - 2\chi\frac{(m^2+n^2)^2}{m^2}}. \tag{33b}$$

With the forms assumed in equations (32) the boundary conditions will be satisfied if the physical wave number in the axial direction is odd, for then

$$\cos m\lambda = \cos\frac{m^*\pi}{2} = 0, \quad m^* = 1,3,5 \ldots \tag{34}$$

Then the first approximations satisfy both the governing equations and the boundary conditions.

If equations (7) are examined with a view towards obtaining the load-shortening relationship, it is found that

$$I_1 \equiv 0, \tag{35}$$

again, for F_1 is still periodic. To obtain I_2, F_2 must be found for it is not yet known whether F_2 will be periodic for the finite shell. If it is, then just w_1,f are needed to calculate I_2.

The details of further calculations are omitted here for the sake of brevity. The second approximations to the stress function, F_2, and the displacement, w_2, are given as

$$\begin{aligned} w_2 = {} & (A \cos 2mx - QR_{10} \cosh q_1 x + P_{20} - \bar{Q}R_{30} \cosh \bar{q}_1 x) + \\ & + (B - QR_{11} \cosh p_1 x - QR_{21} \cosh p_2 x - \bar{Q}R_{31} \cosh \bar{p}_1 x \\ & - \bar{Q}R_{41} \cosh \bar{p}_2 x) \cos 2ny \end{aligned}$$

$$\begin{aligned} F_2 = {} & (C \cos 2mx + R_{10} \cosh q_1 x + R_{20} + R_{30} \cosh \bar{q}_1 x) \\ & + (D + P_{11} \cosh p_1 x + R_{21} \cosh p_2 x + R_{31} \cosh \bar{p}_1 x \\ & + R_{41} \cosh \bar{p}_2 x) \cos 2ny. \end{aligned} \tag{36b}$$

The constants A,B,C,D are given as

$$A = \frac{8\varphi(\alpha_{11}\beta_{11})m^2n^2 + \varphi(\alpha_{11})^2n^2}{8(1-8m^2\chi+16m^4)} \tag{37a}$$

$$B = \frac{\varphi(\alpha_{11}\beta_{11})}{16} \left(\frac{m}{n}\right)^2 \tag{37b}$$

$$C = \frac{8A - \varphi(\alpha_{11})^2 n^2}{32m^2} \tag{37c}$$

$$D = -\frac{\varphi(\alpha_{11})^2}{32}\left(\frac{m}{n}\right)^2 \tag{37d}$$

$$\varphi = [12(1-\nu^2)]^{1/2} \tag{37e}$$

The unknown constants

$$R_{10}, P_{20}, R_{30}, R_{20}, R_{11}, R_{21}, R_{31}, R_{41} \tag{38}$$

are determined by the requirement that the coefficients of each harmonic in the circumferential direction must satisfy the boundary conditions independently. As the assumption of hyperbolic cosines in the axial direction implies symmetry in the axial direction, for each harmonic coefficient four boundary condtions (equations (29)) are available, and four constants have to be determined (equation (38)).

The constants in the arguments of the hyperbolic functions are

$$q_1 = -\frac{1}{\sqrt{2}}\left[(1 - \chi)^{1/2} + i(1 + \chi)^{1/2}\right]$$

$$P_1 \quad \frac{1}{2\sqrt{2}}(\alpha_1 + i\beta_1), \quad P_2 = \frac{1}{2\sqrt{2}}(\alpha_2 + i\beta_2)$$

$$\alpha_1 = -(1-\chi)^{1/2} - (R + 16n^2 - \chi)^{1/2}$$

$$\alpha_2 = +(1-\chi)^{1/2} - (R + 16n^2 - \chi)^{1/2}$$

$$\beta_1 = -(1+\chi)^{1/2} - (R - 16n^2 + \chi)^{1/2}$$

(Continued)

$$\beta_2 = + (1+\chi)^{1/2} - (R - 16n^2 + \chi)^{1/2}$$

$$R = + (1 - 32\chi n^2 + 256n^4)^{1/2} \qquad (39)$$

The details of obtaining these expressions and the homogeneous solutions to the linearized coupled Donnell equations are given in the Appendix.

Returning again to equations (7) it is apparent that enough information has been obtained to compute I_2. Not quite so readily apparent is the fact that I_3 will be identically zero; this result will now be proven. The solutions already obtained are in the form

$$w_1 = \alpha_{11} \cos mx \cos ny$$

$$F_1 = \beta_{11} \cos mx \cos ny$$

$$w_2 = A(x) + B(x) \cos 2ny$$

$$F_2 = C(x) + D(x) \cos 2ny.$$

Substitution of these into equations (8c) readily shows that w_3, F_3 will be of the form

$$w_3 = E(x) \cos ny + F(x) \cos 3ny$$

$$F_3 = G(x) \cos ny + H(x) \cos 3ny.$$

If the above expressions are substituted into equation (7c), and use is made of orthogonality and periodicity, then it can be shown that

$$I_3 \equiv 0.$$

Then the load-shortening relationship can be written as

$$\rho = \chi + e^2 I_2 + O(e^4) \qquad (40)$$

Now

$$I_2 = \frac{\sqrt{3(1-\nu^2)}}{\lambda_x \lambda_y} \int_0^{\lambda_y} \int_{-\lambda}^{\lambda} (F_{2,yy} - \nu F_{2,xx} - \frac{\varphi}{2} w_{1,x}^2 + \frac{\varphi}{2} f_{,x}^2)\, dxdy .$$

Substitution of the expressions already obtained for F_2, w_1 and f yields, after some manipulation,

$$I_2 = -\frac{3(1-\nu^2)m^2}{4} (\alpha_{11}^2 - \alpha_{11}^{0^2})$$

$$- \frac{2\nu\sqrt{3(1-\nu^2)}}{\lambda} [(a\bar{K}_1 - b\bar{K}_2) \sinh a\lambda \cos b\lambda$$

$$- (a\bar{K}_2 + b\bar{K}_1) \cosh a\lambda \sin b\lambda] , \qquad (41)$$

where

$$a = \frac{1}{\sqrt{2}} (1 - \chi)^{1/2} \qquad (42a)$$

$$b = \frac{1}{\sqrt{2}} (1 + \chi)^{1/2} , \qquad (42b)$$

and

$$\bar{K}_1 = \frac{m^2 \cos 2m\lambda}{ab[\sinh^2 a\lambda + \cos^2 b\lambda]} K_1 \qquad (43a)$$

$$\bar{K}_2 = \frac{m^2 \cos 2m\lambda}{ab[\sinh^2 a\lambda + \cos^2 b\lambda]} K_2 , \qquad (43b)$$

with

$$K_1 = J_1 \sinh a\lambda \sin b\lambda - J_2 \cosh a\lambda \cos b\lambda \qquad (43c)$$

$$K_2 = J_1 \cosh a\lambda \cos b\lambda + J_2 \sinh a\lambda \sin b\lambda , \qquad (43d)$$

where

$$J_1 = (2X^2C - AX - C) \tag{43e}$$

$$J_2 = (1 - X^2)^{1/2}(2XC - A), \tag{43f}$$

and A, C, α_{11}, β_{11}, have been previously defined.

Thus the load-end-shortening relationship has been obtained as a function of four geometric parameters: the imperfection amplitude e, the reduced axial wave number m, the reduced circumferential wave number n, and the dimensionless shell half-length λ. In terms of physical quantities these last three parameters are

$$\lambda = [12(1-\nu^2)]^{1/4} \frac{L}{\sqrt{Rt}}$$

$$n = \frac{n^*}{[12(1-\nu^2)]^{1/4}} \sqrt{\frac{t}{R}}$$

$$m = \frac{m^*\pi}{2[12(1-\nu^2)]^{1/4}} \frac{\sqrt{Rt}}{L} .$$

Numerical calculations have been carried out to determine the effect of e,m,n,λ on the buckling load; the results are given in Tables 6 through 9 and in Figures 6 and 7.

The data presented in Table 6 illustrate the variation of the maximum load with the amplitude of the imperfection parameter. As would be expected from an examination of the results obtained for the infinite shell, the load-carrying capacity of the shell decreases as the initial deviation from straightness increases.

Tables 7, 8, 9 are presented to show the variation in maximum load with the length to radius ratio, and with the number of circumferential buckles. The imperfection parameter was fixed at $e = 0.10$, and the radius-to-thickness ratio was taken as 625, while the half-length-to-radius ratio was taken as $1/2$, 1, 2 in Tables 7, 8, 9 respectively. Then the number of axial half wave-lengths(m^*) was varied subject only to the restrictions that m^* must be odd for the satisfaction of boundary coditions, and that the reduced wave number m could never be greater than unity. This last restriction arises from the following condition between the axial wave number m and the circumferential wave number n:

$$\frac{(m^2 + n^2)^2}{m^2} = 1 . \tag{44}$$

This condition assures buckling at the classical critical load for a perfect shell.

It is seen from these three tables that the lowest buckling load for each occurs with the maximum possible number of axial waves. These results are summarized as follows:

L/R	m^*	n^*	ρ
0.50	13	13.71	0.672
1.00	27	11.34	0.664
2.00	57	5.51	0.652

This small chart indicates that as the length-to-radius ratio is increased, there is a small drop in the buckling load, and a sharper drop in the number of circumferential buckles.

In Figures 6 and 7 curves of maximum load ratio ρ_{max} vs the dimensionless half-length λ are plotted, for various values of m,n. Again for any particular value of m,n, the length effect is relatively small. In addition, as was noted above, the load decreases as m increases and n decreases.

CONCLUSIONS

This report has been concerned with presenting a somewhat different approach to one of the most exciting problems of elasticity theory, the buckling of thin circular cylindrical shells under axial compression. The particular advantage in the perturbation scheme used here is that the tools of linear mathematics are now applicable to the problem. The major drawback is that it is difficult to pin down the exact validity of all the numerical results obtainable.

As far as the physics of the problem is concerned, a few interesting trends have been developed. First it was shown that, as might be expected, a shell that is manufactured with smaller geometric imperfections will be able to support more load. However, when loss of stability does occur for a nearly perfect shell, the failure is more likely to be catastrophic, for it has been shown that the increase in the displacements is much more rapid for shells with small eccentricities. In addition it was demonstrated that axisymmetric imperfections seem to be the most dangerous to the load carrying capability of the shell.

For shells of finite length, it appears that there is no appreciable length effect. The load does drop somewhat as the length of the shell increases, but the only rapid change occurs in the number of circumferential buckles. It would seem that the longer the shell, the smaller the number of such buckles.

REFERENCES

1. Lorenz, R., Achsensymmetrische Verzerrungen in dünnwandigen Hohlzylindern, Zeitschrift des Vereins Deutscher Ingenieure, Vol. 52, No. 43, p. 1706, October 1908.

2. Timoshenko, S., Einige Stabilitätsprobleme der Elastizitätstheorie, Zeitschrift für Mathematik und Physik, Vol. 58, No. 4, p. 337, June 1910.

3. Southwell, R. V., On the General Theory of Elastic Stability, Philosphical Transactions of the Royal Society, London, Series A, Vol. 213, No. A501, p. 187, August 1913.

4. Flügge, W., Die Stabilität der Kreiszylinderschale, Ingenieur-Archiv, Vol. 3, No. 5, p. 463, December 1932.

5. Donnell, L. H., A New Theory for the Buckling of Thin Cylinders under Axial Compression and Bending, Transactions of the American Society of Mechanical Engineers, Report AER-56-12, Vol. 56, p. 795, 1934.

6. Kármán, Th. von, and Tsien, Hsue-Shen, The Buckling of Thin Cylindrical Shells under Axial Compression, Journal of the Aeronautical Sciences, Vol. 8, No. 8, p. 303, June 1941.

7. Hoff, Nicholas J., The Perplexing Behavior of Thin Cylindrical Shells in Axial Compression, Second Theodore von Kármán Memorial Lecture of the Israel Society of Aeronautical Sciences, Israel Journal of Technology, Vol. 4, No. 1, p. 1, February 1966.

8. Donnell, L. H., and Wan, C. C., Effect of Imperfections on Buckling of Thin Cylinders and Columns under Axial Compression, Journal of Applied Mechanics, Vol. 17, No. 1, p. 73, March 1950.

9. Loo, T. T., Effects of Large Deflections and Imperfections on the Elastic Buckling of Cylinders under Torsion and Axial Compression, Proceedings of the Second U. S. Congress of Applied Mechanics, 1954, p. 345.

10. Lee, L. H. N., Effects of Modes of Initial Imperfections on the Stability of Cylindrical Shells under Axial Compression, Collected Papers on Instability of Shell Structures - 1962, NASA TN D-1510, Washington, D. C., 1962, p. 143.

11. Sobey, A. J., The Buckling of an Axially Loaded Circular Cylinder with Initial Imperfections, Royal Aeronautical Establishment Report No. 64016, September 1964.

12. Madsen, W. A., and Hoff, Nicholas J., The Snap-Through and Post-buckling Equilibrium Behavior of Circular Cylindrical Shells under Axial Load, Stanford University Department of Aeronautics and Astronautics Report SUDAER No. 227, April 1965.

13. Almroth, B. O., Influence of Imperfections and of Edge Restraint on the Buckling of Axially Compressed Cylinders, Lockheed Missles and Space Company Report 6-75-65-57, 1965.

14. Koiter, W. T., The Effect of Axisymmetric Imperfections on the Buckling of Cylindrical Shells under Axial Compression, Proceedings of the Royal Netherlands Academy of Sciences, Amsterdam, Series B, Vol. 66, No. 5, 1963.

15. Koiter, W. T., Over de Stabiliteit van het elastisch Evenwicht, H. J. Paris, Amsterdam, Holland, 1945.

16. Koiter, W. T., Elastic Stability and Postbuckling Behavior, Proceedings of the Symposium on Non-Linear Problems, edited by R. E. Langer, University of Wisconsin Press, 1963, p. 257.

17. Mayers, J., and Rehfield, L., Further Nonlinear Considerations in the Buckling of Axially Compressed Circular Cylindrical Shells, Stanford University Department of Aeronautics and Astronautics Report SUDAER No. 197, June 1964.

18. Van Dyke, Milton, Perturbation Methods in Fluid Mechanics, Academic Press, New York, 1964.

19. Stein, Manuel, Loads and Deformations of Buckled Rectangular Plates, National Aeronautics and Space Administration, Technical Report R-40, 1959.

20. Kaplan, A., and Fung, V. C., A Nonlinear Theory of Bending and Buckling of Thin Elastic Shallow Shells, National Advisory Committee for Aeronautics Technical Note 3212, 1954.

21. Hoff, Nicholas J., Low Buckling Stresses of Axially Compressed Circular Cylindrical Shells of Finite Length, Stanford University Department of Aeronautics and Astronautics Report SUDAER No. 192, July 1964.

22. Hoff, Nicholas J., and Soong, Tsia-Chen, Buckling of Circular Cylindrical Shells in Axial Compression, Stanford University Department of Aeronautics and Astronautics Report SUDAER No. 204, August 1964.

APPENDIX

SOLUTIONS TO THE COUPLED, HOMOGENEOUS DONNELL EQUATIONS

The purpose of this Appendix is to outline briefly the determination of the characteristic roots and the form of the solutions to the coupled, homogeneous, Donnell equations:

$$\nabla^4 w + 2\chi w_{,xx} - F_{,xx} = 0$$

$$\nabla^4 F + w_{,xx} = 0 \quad .$$

Since only those solutions are of interest that are symmetric about the centerline of the shell ($x = 0$), it can be assumed that the stress function F and the displacement w are of the form

$$F = R \cosh px \cos ny$$

$$w = P \cosh px \cos my \quad ,$$

where P, R are arbitrary constants. Substitution into the differential equations yields the following two algebraic equations:

$$[(p^2 - n^2)^2 + 2\chi p^2]P - p^2 R = 0$$

$$p^2 P + (p^2 - n^2)^2 R = 0 \quad .$$

For the existence of a non-trivial solution, the determinant of the coefficients of the above algebraic equations must vanish. This yields the characteristic equation for the roots

$$(p^2 - n^2)^4 + 2\chi p^2 (p^2 - n^2) + p^4 = 0 \quad .$$

The eight roots of this equation have been obtained previously in closed form in work done at Stanford University on the stability limits of shells

of finite length (see, for example, Hoff [21]). They can be written in the form

$$p_1 = \frac{1}{2\sqrt{2}}(\alpha_1 + \beta_1), \quad p_2 = \frac{1}{2\sqrt{2}}(\alpha_2 + i\beta_2)$$

$$p_3 = \bar{p}_1, \; p_4 = \bar{p}_3$$

$$p_5 = -p_2, \; p_6 = -p_1$$

$$p_7 = \bar{p}_2, \; p_8 = -\bar{p}_1 \; ,$$

where

$$\alpha_1 = -(1 - \chi)^{1/2} - (R + 4n^2 - \chi)^{1/2}$$

$$\alpha_2 = +(1 - \chi)^{1/2} - (R + 4n^2 - \chi)^{1/2}$$

$$\beta_1 = -(1 + \chi)^{1/2} - (R - 4n^2 + \chi)^{1/2}$$

$$\beta_2 = +(1 + \chi)^{1/2} - (R - 4n^2 + \chi)^{1/2}$$

$$R = +(1 - 8n^2\chi + 16n^4)^{1/2}.$$

Thus the solutions can be written as

$$w = \sum_{i=1}^{8} P_i \cosh p_i x \cos ny$$

$$F = \sum_{i=1}^{8} R_i \cosh p_i x \cos ny \; .$$

As the hyperbolic cosine is a symmetric function, and since the roots p_5, p_6, p_7, p_8 are just the negatives of p_1, p_2, p_3, p_4, these solutions can

actually be written as

$$w = \sum_{i=1}^{4} P_i \cosh p_i x \cos ny$$

$$F = \sum_{i=1}^{4} R_i \cosh p_i x \cos ny \ .$$

The boundary conditions, enforced at $x = + \lambda$, are then automatically satisfied at $x = - \lambda$.

Finally, it will be recalled that only four boundary conditions should be stipulated, while it appears that there are actually eight arbitrary constants:

$$P_1, P_2, P_3, P_4; \quad R_1, R_2, R_3, R_4 \ .$$

In fact, these constants are related, and this relationship is determined by substitution of the forms of the solutions for the displacement w and the stress function F into either of the two differenetial equations. In this manner one obtains

$$P_1 = - QR_1, \quad P_2 = - QR_2$$

$$P_3 = - \bar{Q}R_3, \quad P_4 = - \bar{Q}R_4 \ ,$$

where

$$Q = - X + 1(1 - X^2)^{1/2}.$$

Thus the two solutions can be written as

$$w = - (QR_1 \cosh p_1 x + QR_2 \cosh p_2 x + \bar{Q}R_3 \cosh p_3 x + \bar{Q}R_4 \cosh p_4 x) \cos ny$$

$$F = \sum_{i=1}^{4} R_i \cosh p_i x \cos ny \ .$$

For the case when the deformation is axisymmetric, that is when $n = 0$, the two solutions become

$$w = P_1 \cosh p_1 x + P_2 + P_3 \cosh p_3 x + P_4 x^2$$

$$F = R_1 \cosh p_1 x + R_2 + R_3 \cosh p_3 x + R_4 x^2 .$$

The constant and quadratic terms in each expression are due to the repeated root $p = 0$. Substitution into either of the differential equations yields:

$$w = - (QR_1 \cosh p_1 x - P_2 + \bar{Q}R_3 \cosh p_3 x)$$

$$F = R_1 \cosh p_1 x + R_2 + R_3 \cosh p_3 x \ .$$

TABLE 1. VARIATION OF MAXIMUM LOAD RATIO ρ_{max} WITH THE NUMRER OF TERMS IN THE LOAD-SHORTENING RELATIONSHIP; INFINITE SHELL; $\alpha_{20}^{0} = 0.25$

e	ONE TERM	TWO TERMS	THREE TERMS
10^{-4}	0.996	0.994	0.992
10^{-3}	0.986	0.976	0.971
10^{-2}	0.944	0.911	0.894
10^{-1}	0.742	0.649	0.610
0.3	0.485	0.352	0.314
0.5	0.307	0.173	0.151
0.7	0.179	0.0637	0.0561
0.8	0.129	0.0302	0.0284
0.9	0.0888	0.00941	0.0107

$$w_0 = e(\alpha_{11}^{0} \cos mx \cos ny + \alpha_{20}^{0} \cos 2mx)$$

$$m = n = 1/2, \quad \alpha_{11}^{0} = 1.00, \quad \alpha_{20}^{0} = 0.25, \quad \nu = 0.30$$

TABLE 2. COMPARISON OF MAXIMUM LOAD RATIO ρ_{max} AND END-SHORTENING PARAMETER X FOR DIFFERENT APPROXIMATIONS TO LOAD-SHORTENING RELATION.

	ONE TERM		TWO TERMS		THREE TERMS	
e	X	ρ	X	ρ	X	ρ
10^{-4}	0.996+	0.996	0.994+	0.994	0.993	0.992
10^{-3}	0.990	0.986	0.981	0.976	0.973	0.971
10^{-2}	0.961	0.944	0.928	0.911	0.907	0.894
10^{-1}	0.825	0.742	0.745	0.649	0.676	0.610
0.3	0.644	0.485	0.488	0.352	0.429	0.314
0.5	0.495	0.307	0.310	0.173	0.264	0.151
0.7	0.363	0.179	0.180	0.0637	0.149	0.0561
0.8	0.314	0.129	0.120	0.0302	0.0990	0.0284
0.9	0.248	0.0888	0.0599	0.00941	0.0660	0.0107

$$w_0 = e(\alpha_{11}^0 \cos mx \cos ny + \alpha_{20}^0 \cos mx)$$

$$m = n = 1/2, \quad \alpha_{11}^0 = 1.00, \quad \alpha_{20}^0 = 0.25, \quad \nu = 0.30$$

TABLE 3. COMPARISON OF DISPLACEMENTS AT MAXIMUM LOAD

e	X	$\frac{ew_2}{w_1}$	$\frac{ew_3}{w_2}$	w
10^{-4}	0.974	0.097	0.193	0.00554
	0.990	0.828	1.653	0.04628
	(M) 0.993	1.631	3.256	0.161
10^{-3}	0.941	0.179	0.353	0.0267
	0.957	0.352	0.696	0.0479
	(M) 0.973	0.971	1.929	0.191
10^{-2}	0.875	0.382	0.738	0.167
	0.892	0.512	0.994	0.234
	(M) 0.907	0.720	1.404	0.374
10^{-1}	0.644	0.392	0.702	0.586
	0.660	0.438	0.790	0.658
	(M) 0.676	0.492	0.892	0.748
0.3	0.396	0.284	0.438	0.875
	0.413	0.310	0.486	0.933
	(M) 0.429	0.339	0.538	1.000
0.5	0.231	0.183	0.213	0.993
	0.248	0.203	0.249	1.042
	(M) 0.264	0.225	0.287	1.095
0.7	0.116	0.101	0.0334	1.093
	0.132	0.119	0.0646	1.136
	(M) 0.149	0.139	0.0972	1.184
0.8	0.0660	0.0605	-0.0534	1.132
	0.0826	0.0778	-0.0246	1.173
	(M) 0.0990	0.0962	0.0061	1.218
0.9	0.0330	0.0321	-0.1191	1.196
	0.0495	0.0496	-0.0905	1.237
	(M) 0.0660	0.0680	-0.0600	1.282

(M) denotes point where maximum load occurs.

$$w_0 = e(\alpha^0_{11} \cos mx \cos ny + \alpha^0_{20} \cos 2mx)$$

$$\alpha^0_{11} = 1.00, \quad \alpha^0_{20} = 0.25, \quad m = n = 1/2, \quad \nu = 0.30$$

TABLE 4. COMPARISON OF POTENTIAL ENERGY OF VARIOUS APPROXIMATIONS UP TO MAXIMUM LOADS.

e	X	$U_{(0)}$	$U_{(1)}$	$U_{(2)}$	$U_{(3)}$
0	1.000	0.184	0.184	0.184	0.184
10^{-4}	0.993	0.181	0.181	0.181	0.181
10^{-3}	0.973	0.174	0.174	0.174	0.174
10^{-2}	0.907	0.151	0.151	0.151	0.151
10^{-1}	0.676	0.0840	0.0827	0.0820	0.0815
0.3	0.429	0.0338	0.0311	0.0294	0.0288
0.5	0.264	0.0128	0.0106	0.00910	0.00882
0.7	0.149	0.00405	0.00286	0.00198	0.00195
0.8	0.0990	0.00180	0.00114	0.000639	0.000641
0.9	0.0660	0.00080	0.000445	0.000152	0.000179

$$w_0 = e(\alpha^0_{11} \cos mx \cos ny + \alpha^0_{20} \cos 2mx)$$

$$m = n = 1/2, \quad \alpha^0_{11} = 1.00, \quad \alpha^0_{10} = 0.25, \quad \nu = 0.30$$

$$U_{(m)} = U_0 + eU_1 + \ldots + e^m U_m$$

TABLE 5. VARIATION OF MAXIMUM LOAD RATIO ρ_{max} WITH THE NUMBER OF TERMS IN THE LOAD-SHORTENING RELATIONSHIP; INFINITE SHELL; $\alpha_{20}^{0} = 0.00$

e	ONE TERM	THREE TERMS
10^{-4}	0.996	0.994
10^{-3}	0.990	0.976
10^{-2}	0.948	0.914
10^{-1}	0.774	0.680
0.3	0.545	0.432
0.5	0.382	0.281
0.7	0.258	0.180
0.8	0.206	0.143
0.9	0.161	0.113

$$w_0 = e(\alpha_{11}^{0} \cos mx \cos ny + \alpha_{20}^{0} \cos 2mx)$$

$m = n = 1/2$, $\alpha_{11}^{0} = 1.00$, $\alpha_{20}^{0} = 0.00$, $\nu = 0.30$

TABLE 6. INFLUENCE OF IMPERFECTION SIZE ON MAXIMUM LOAD RATIO OF FINITE LENGTH SHELL

λ	e	ρ
1.745	0.10	0.634
	0.010	0.99+
	0.0010	0.99+
26.180	0.10	0.672
	0.010	0.928
	0.0010	0.99+
99.484	0.10	0.671
	0.010	0.928
	0.0010	0.99+

$$w_0 = e\,\alpha_{11}^0 \cos mx \cos ny$$

$$m = 0.900, \quad n = 0.300, \quad \alpha_{11}^0 = 1, \quad \upsilon = 0.30$$

TABLE 7. VARIATION OF MAXIMUM LOAD RATIO ρ_{max} WITH NUMBER OF BUCKLES; L/R = 0.50

m*	n*	m	n	ρ
1	11.53	0.069	0.254	0.939
3	18.42	0.207	0.405	0.872
5	21.61	0.346	0.476	0.822
7	22.71	0.484	0.500	0.786
9	22.03	0.622	0.485	0.747
11	19.40	0.760	0.427	0.708
13	13.71	0.899	0.302	0.672

e = 0.10, R/t = 625, L/R = 0.50, λ = 22.72

TABLE 8. VARIATION OF MAXIMUM LOAD RATIO ρ_{max} WITH NUMBER OF BUCKLES; L/R = 1.00

m*	n*	m	n	ρ
1	8.30	0.0346	0.183	0.961
3	13.86	0.104	0.305	0.920
5	17.18	0.173	0.378	0.888
7	19.46	0.242	0.428	0.860
9	21.04	0.311	0.463	0.835
11	22.06	0.380	0.485	0.812
13	22.61	0.449	0.497	0.793
15	22.71	0.518	0.500	0.774
17	22.37	0.588	0.492	0.754
19	21.58	0.657	0.475	0.734
21	20.27	0.726	0.446	0.716
23	18.35	0.795	0.404	0.697
25	15.57	0.864	0.343	0.680
27	11.34	0.933	0.250	0.664

e = 0.10, R/t = 625, L/R = 1.00, λ = 45.45

TABLE 9. VARIATION OF MAXIMUM LOAD RATIO ρ_{max} WITH NUMBER OF BUCKLES; L/R = 2.00

m*	n*	m	n	ρ
1	5.92	0.0173	0.130	0.975
5	12.77	0.0864	0.281	0.930
9	16.47	0.156	0.362	0.896
13	18.97	0.225	0.417	0.867
17	20.70	0.294	0.455	0.841
21	21.85	0.363	0.481	0.818
25	22.51	0.432	0.495	0.797
29	22.72	0.501	0.500	0.777
33	22.50	0.570	0.495	0.757
37	21.82	0.639	0.480	0.738
41	20.65	0.708	0.454	0.719
45	18.90	0.778	0.416	0.701
49	16.37	0.847	0.360	0.684
53	12.61	0.916	0.277	0.668
57	5.51	0.985	0.121	0.652

e = 0.10, R/t = 625, L/R = 2.00, λ = 90.89

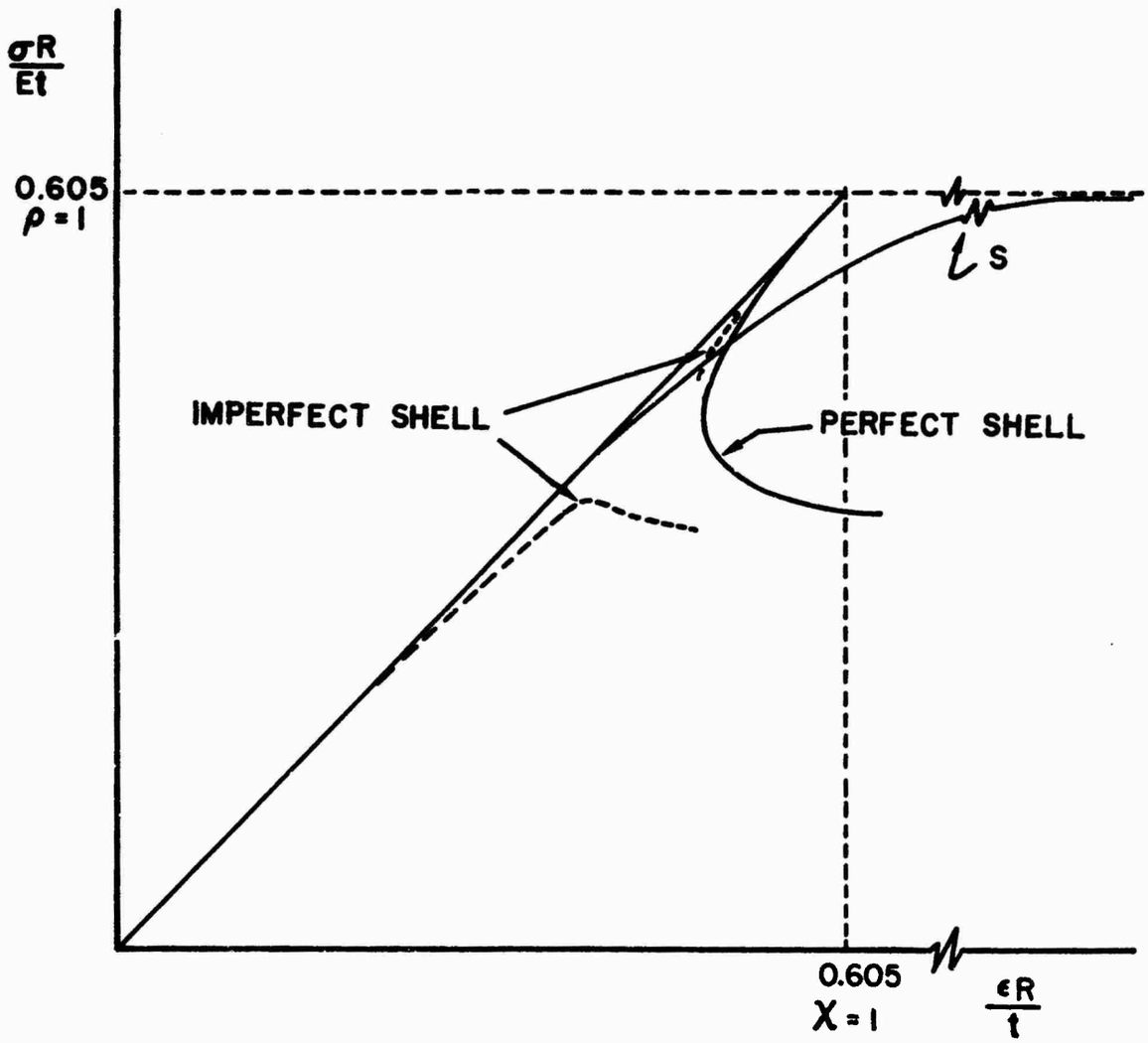

Figure 1. Generalized Load vs End Shortening

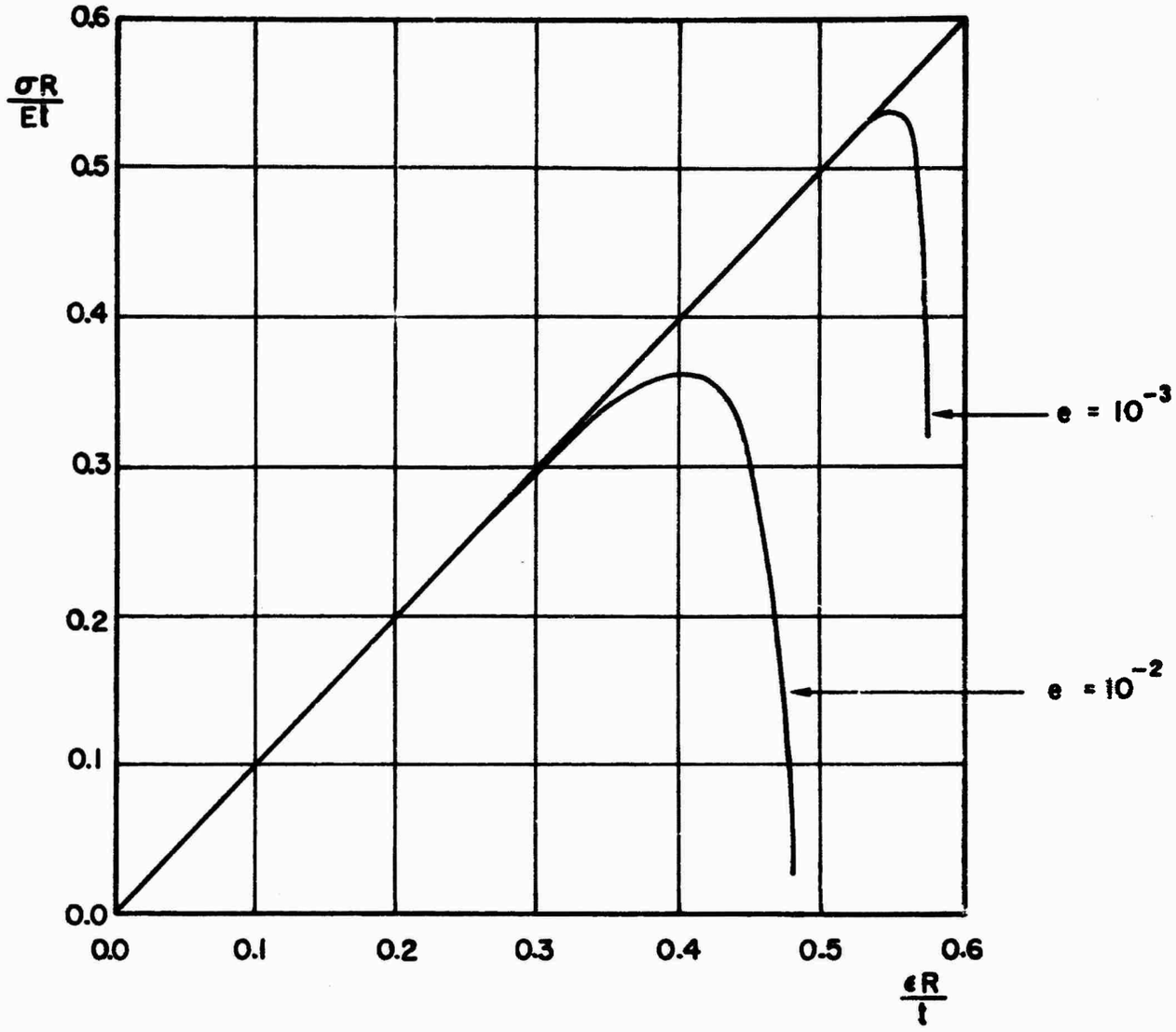

Figure 2. Typical Load-Shortening Curves

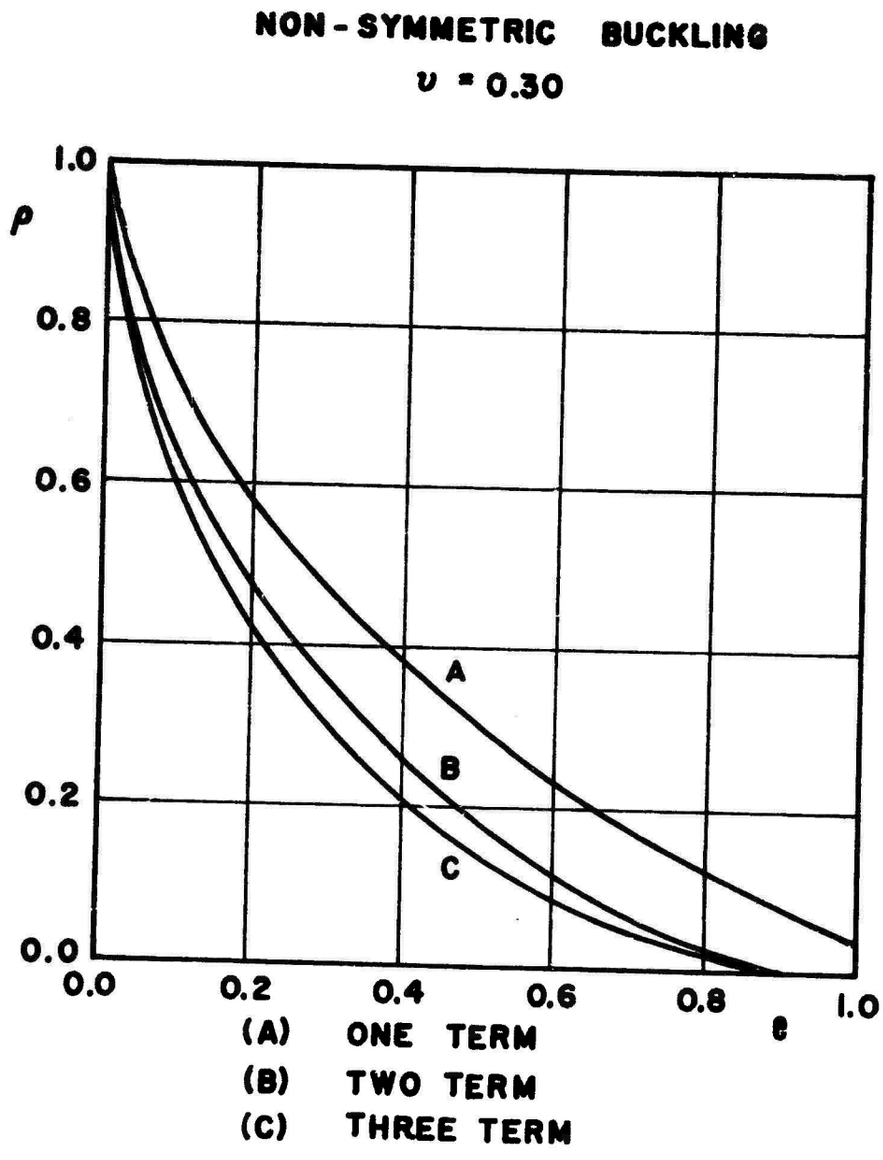

Figure 3. Maximum Load Ratio p_{max} vs Imperfection Amplitude; Non-Symmetric Buckling

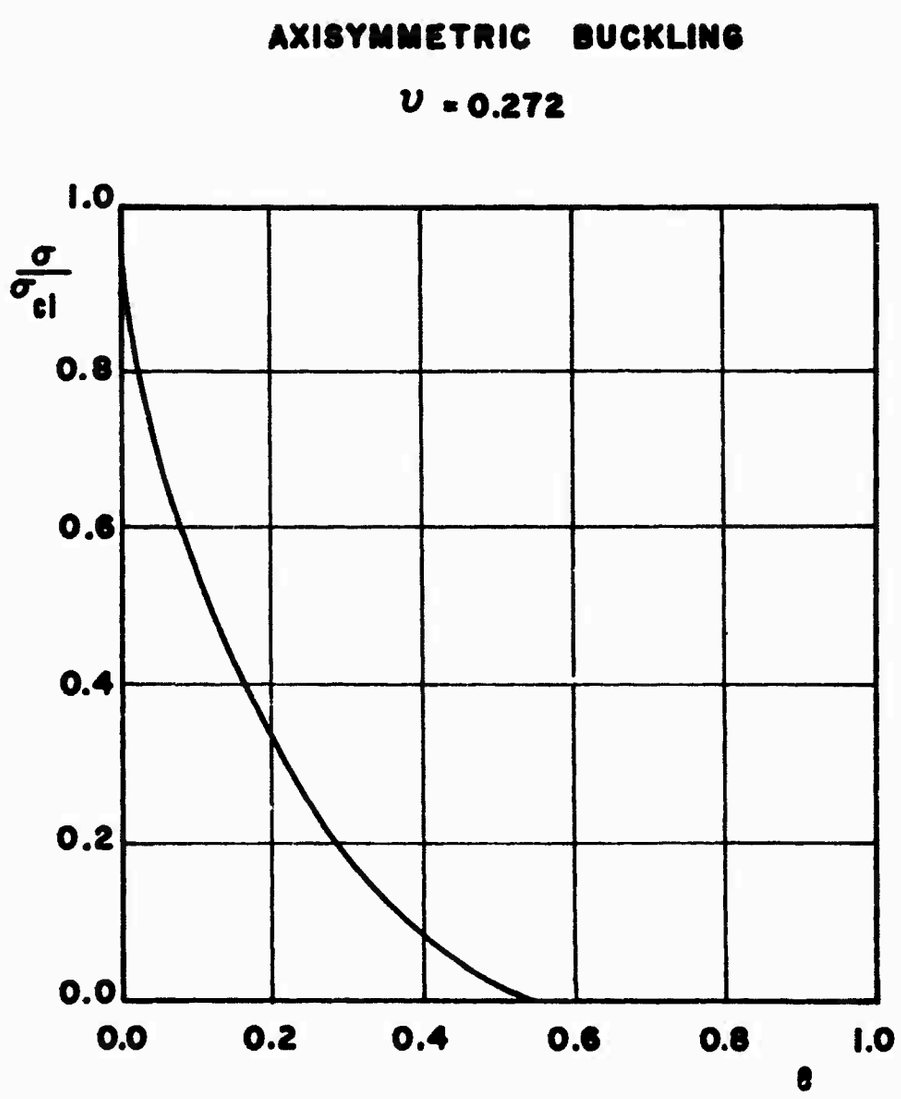

Figure 4. Maximum Load Ratio ρ_{max} vs Imperfection Amplitude; Axisymmetric Buckling

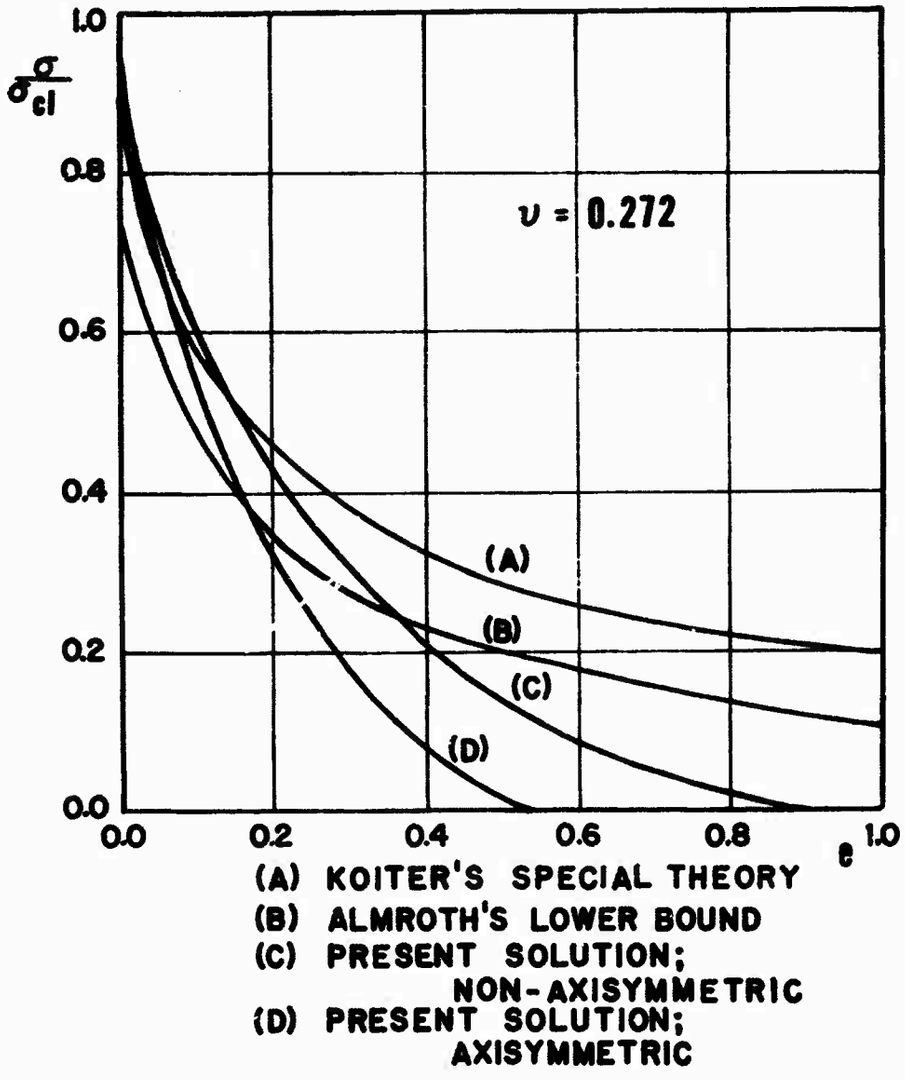

Figure 5. Maximum Load Ratio ρ_{max} vs Imperfection Amplitude; Comparison with the Results of Koiter and Almroth

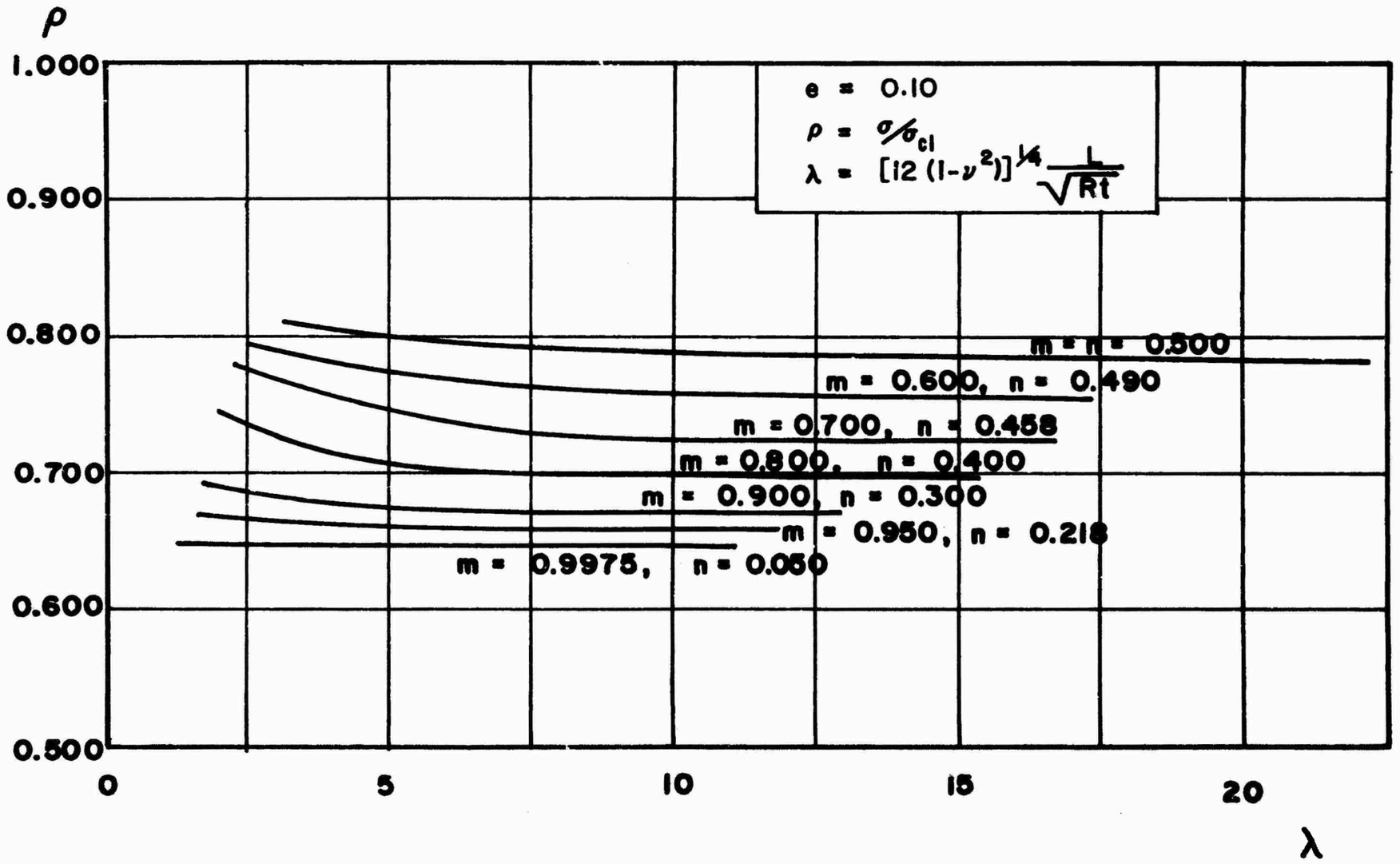

Figure 6. Maximum Load Ratio ρ_{max} vs Half-Length λ

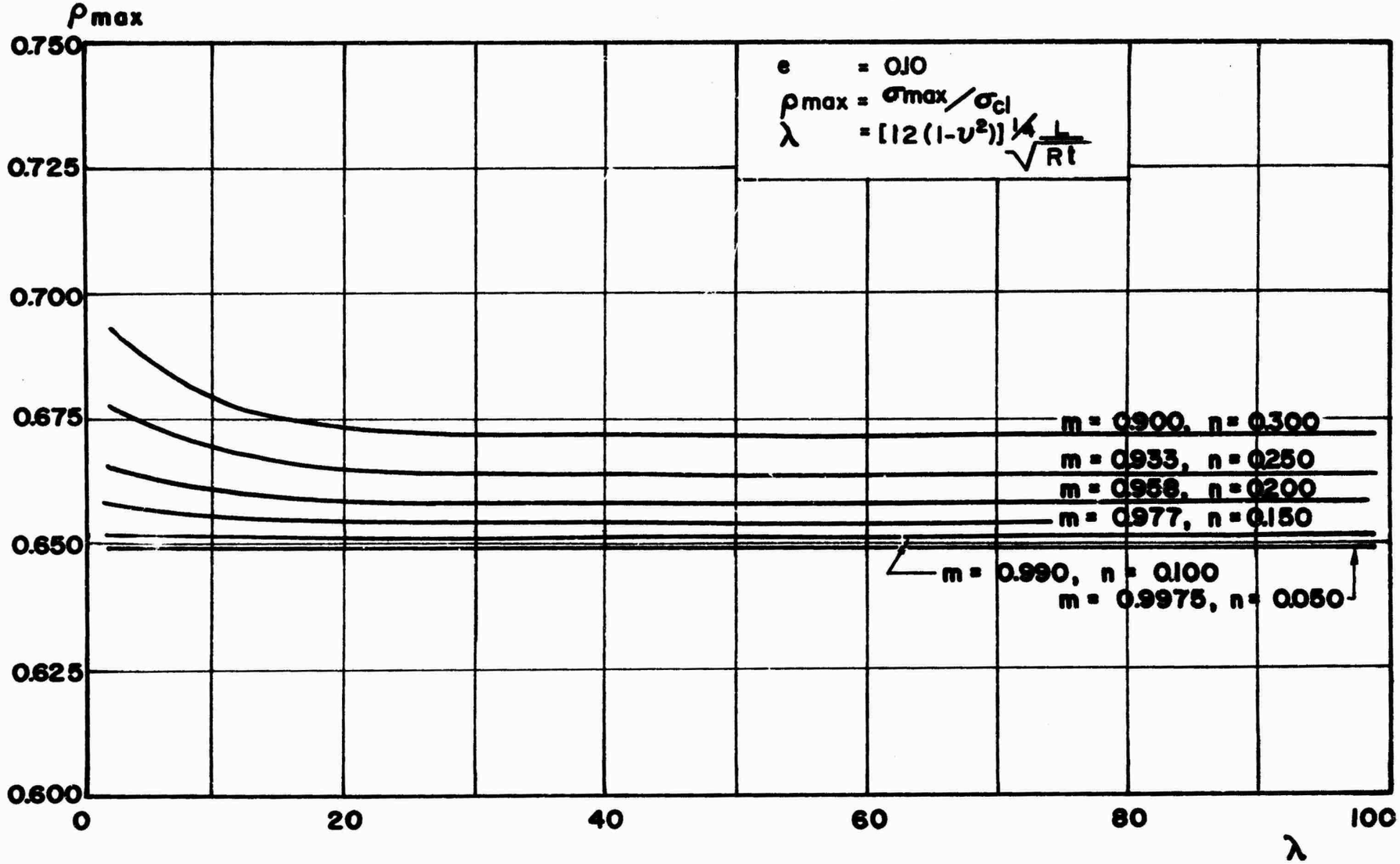

Figure 7. Maximum Load Ratio ρ_{max} vs Half-Length λ

Security Classification

DOCUMENT CONTROL DATA - R & D

(Security classification of title, body of abstract and indexing annotation must be entered when the overall report is classified)

1. ORIGINATING ACTIVITY (Corporate author)

Stanford University
Department of Aeronautics and Astronautics
Stanford, California 94305

2a. REPORT SECURITY CLASSIFICATION

UNCLASSIFIED

2b. GROUP

3. REPORT TITLE

PERTURBATION SOLUTIONS FOR THE BUCKLING PROBLEM OF AXIALLY COMPRESSED THIN CYLINDRICAL SHELLS

4. DESCRIPTIVE NOTES (Type of report and inclusive dates)

Scientific Interim

5. AUTHOR(S) (First name, middle initial, last name)

Clive L. Dym
Nicholas J. Hoff

6. REPORT DATE

July 1966

7a. TOTAL NO. OF PAGES

63

7b. NO. OF REFS

22

8a. CONTRACT OR GRANT NO.

AF 49(638)1276

b. PROJECT NO. 9782-01

c. 61445014

d. 681307

9a. ORIGINATOR'S REPORT NUMBER(S)

SUDAAR No. 282

9b. OTHER REPORT NO(S) (Any other numbers that may be assigned this report)

AFOSR-66-1755

10. DISTRIBUTION STATEMENT

1. Distribution of this document is unlimited

11. SUPPLEMENTARY NOTES

12. SPONSORING MILITARY ACTIVITY

AF Office of Scientific Research (SREM)
1400 Wilson Boulevard
Arlington, Virginia 22209

13. ABSTRACT

A study is made of the effect of initial deviations on the load carrying capacity of thin circular cylindrical shells under uniform axial compression. A perturbation expansion is used to reduce the nonlinear equations of von Kármán-Donnell to an infinite set of linear equations, of which only the first few need be solved to obtain a reasonable accurate solution. The results for both infinite shells and shells of finite length indicate that a small imperfection can sharply reduce the maximum load that a thin-walled cylinder will sustain. In addition, for a particular set of boundary conditions, it is shown that the effect of the length for a finite shell, is small.

DD FORM 1 NOV 65 1473

Security Classification

Security Classification

14 KEY WORDS	LINK A		LINK B		LINK C	
	ROLE	WT	ROLE	WT	ROLE	WT
Perturbation Solutions Stability of Thin-walled Circular Cylindrical Shells End-condition Effects in Shell Buckling Inaccurate Shell Behavior						